Structure of nanometer-sized polycrystalline iron investigated by positron lifetime spectroscopy

H.-E. Schaefer and R. Würschum
Institut für Theoretische und Angewandte Physik der Universität Stuttgart, Postfach 80 11 40, 7000 Stuttgart 80, West Germany

R. Birringer and H. Gleiter
Institut für Werkstoffwissenschaften der Universität des Saarlandes, Fachbereich 12.1, 6600 Saarbrücken, West Germany
(Received 11 January 1988)

Nanometer-sized polycrystalline materials are polycrystals prepared by compacting very small crystallites (5–10 nm in diameter) under high pressures. The initial studies of Gleiter and co-workers indicate a wide distribution of interatomic distances within the disordered intercrystalline phase, which can be investigated accurately due to its high relative volume fraction in these materials. In the present paper the investigation of nanometer-sized Fe polycrystals by positron lifetime spectroscopy is reported. The influence of the compacting pressure and thermal annealing was studied. The positron lifetimes $\tau_1 = 180 \pm 15$ ps, $\tau_2 = 360 \pm 30$ ps, and long-lived components between 1 and 5 ns, have been observed with saturation trapping of positrons. These values are different from the positron lifetimes in well-annealed bulk iron, in amorphous iron alloys, or in the uncompacted fine nanometer-sized iron crystals ($\tau = 443$ ps). Based on the present results the lifetime τ_1 in nanometer-sized Fe polycrystals is attributed to positron trapping in vacancy-size free volumes in the crystallite interfaces. This is in agreement with the hypothesis of an interfacial structure with a wide distribution of interatomic distances. The lifetime τ_2 is ascribed to positron annihilation in microvoids at the intersections of interfaces. Hence, positron lifetime spectroscopy on nanometer-sized polycrystalline materials appears to supply a specific tool for studying the interfacial structure of solids. The long-lived components indicate ortho-positronium (*o*-Ps) formation in larger voids.

I. INTRODUCTION

The physical, metallurgical, and chemical potentials of materials are controlled by their microstructural characteristics. In search of novel properties of solid materials, Gleiter and co-workers[1–3] have initiated studies of polycrystals with very small crystallite sizes (5–10 nm) which are called nanometer-sized polycrystalline materials, or, abbreviated, nanocrystalline materials.

From the first experiments[1–3] indication for a disordered structure without atomic short-range order in the interfaces between the small crystallites have been found. This solid state structure which differs substantially from fully periodic crystals or the short-range ordered amorphous materials[4,5] and quasicrystals[6] is expected to show novel physical properties and may promise new applications in materials science and engineering.

In a simple model[3] of a one-component nanocrystalline material, two types of atomic environments and therefore two structural phases may be discerned (see Fig. 1): (i) Atoms *within the crystallites* with distances to the surrounding atoms according to the lattice translation vectors, and (ii) atoms *in the crystallite interfaces* with neighboring atoms from two or more crystallites of random mutual orientation relationships.

Due to the great number of different structures of the interfaces, a wide distribution of interatomic distances in the interfaces is expected. This will manifest itself as a component without atomic short-range order in macroscopically averaging measurements. The structure of this component is stabilized due to the boundary conditions given by the skeleton of the small crystallites.

Assuming an interface thickness of 1–2 nm, the

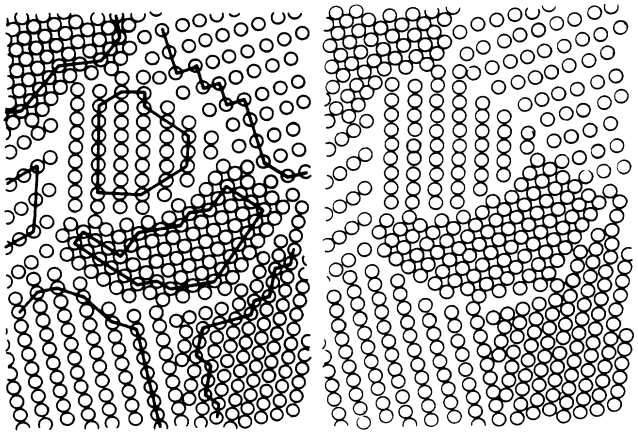

FIG. 1. Simple two-dimensional model of a nanocrystalline material (Ref. 3). The solid line separates the crystalline and the interfacial phase which, in this model, contains one atomic surface layer of the adjoining crystallites without atomic relaxation.

volume fraction of the interfacial component can be estimated as 10–50 % for crystallite sizes between 3 and 10 nm. This makes, in contrast to measurements on conventional polycrystals, precise scattering and material-transport studies on the structure feasible.

Up to now the measuring techniques used to study nanocrystalline materials have been x-ray diffraction with comparative model calculations of the interference function,[7] high-resolution electron microscopy,[3] observation of crystal growth during heat treatment,[8] measurements of the specific heat C_p,[9] and the magnetic susceptibility,[10] as well as Mössbauer spectroscopy.[11]

Positron-annihilation experiments have been performed on fine metal powders since the early applications of this technique in order to study surface states.[12–16]

In the present paper the results of positron lifetime spectroscopy[17,18] on nanometer-sized polycrystalline iron are reported. First results were communicated recently.[19] Positron lifetime spectroscopy is particularly well suited for studying defects in crystals[17,18,20] and structural fluctuations in amorphous materials[21] and can supply an estimate of free volumes in condensed matter.

As we shall see in the following sections, positrons can rapidly escape from the small undisturbed crystallites in the nanocrystalline material because their mean diffusion length is much longer than the crystallite size. When trapped in the disordered interfaces or voids, their lifetimes yield new structural information.

II. EXPERIMENTAL PROCEDURE

A. Preparation of the specimens

The nanocrystals with a mean diameter of 6 nm (Ref. 8) were prepared by using the method of metal evaporation (99.99%-pure Fe) and condensation in a high-purity noble-gas atmosphere.[22,23] After evacuation of the noble gas the fine iron powder was compacted in high vacuum ($p \leq 10^{-3}$ Pa) under various mechanical pressures ($10 \leq p \leq 140$ MPa) to disk-shaped pellets (5 mm in diameter, ~ 0.1 mm thick, density 4 g/cm^3). These pellets were transferred under high vacuum into a glass vial which was melted off from the recipient in order to transport the pellets to the positron laboratory.

For applying higher pressures up to 4.5 GPa the pellets were transferred from the first compacting stage under high vacuum to a second stage. These highly compacted pellets (6 mm in diameter, 50 μm thick, density about 6.3 g/cm^3) were filled under atmospheric pressure into a transport vial which finally was evacuated. No chemical change due to gas penetration into the 4.5-GPa pellets could be observed by Mössbauer spectroscopy. By mass spectrometry, electron spectroscopy for chemical analysis (ESCA), and atomic-absorption analysis an impurity concentration of less than 0.5 wt. % has been determined.[3]

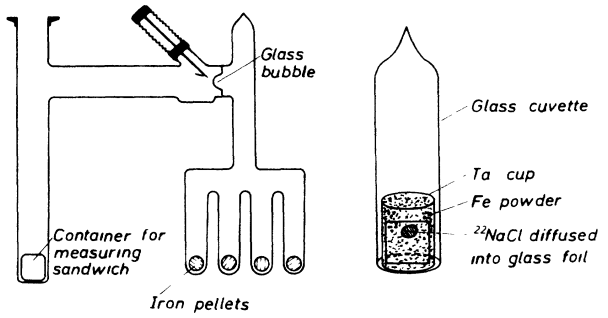

FIG. 2. High vacuum transfer of the iron pellets from the transport glass vial to the measuring vial where they are assembled with the positron source to the measuring sandwich (left-hand side). On the right-hand side the glass vial for positron lifetime measurements on uncompacted iron powder is shown. The ^{22}NaCl positron source was prepared on a glass foil according to Dézsi *et al.* (Ref. 24).

In the positron laboratory the pellets were transferred under high vacuum into the measuring vial (see Fig. 2), where the positron source (activity 1.3×10^6 Bq of ^{22}NaCl packed in a 0.8-μm-thick Al foil) was located between two pellets on each side. Finally, well-annealed polycrystalline iron disks (100 μm thick) were positioned on each face of the sandwich in order to detect, by their short lifetimes, those positrons which could escape from the pellets. For the measurements and the annealing treatments the glass vial (Fig. 2) containing the source-specimen sandwich was melted off under high vacuum.

For comparative measurements uncompacted iron nanocrystals ("iron powder") were transferred under high vacuum in the same manner as the pellets into a glass vial (Fig. 2) which contained a well-annealed Ta cup (wall thickness 0.1 mm) with a positron source (^{22}NaCl, 1.3×10^6 Bq) diffused into a thin (1 mg/cm^2) Jena-glass foil.[24] In this arrangement it is estimated that 96% of the positrons are annihilated within the powder assuming a volume density of 0.23 g/cm^3.

For measurements of the bulk lifetime τ_f in iron, a coarse-grained polycrystalline hollow Fe cylinder was machined from the same material as used for the preparation of the nanocrystals. After etching and annealing (5 h at 1000 °C) the ^{22}NaCl positron source (0.15×10^6 Bq) was deposited in the specimen hole.

The positron lifetime spectra were measured at am-

TABLE I. Type and size of the scintillators, as well as time resolutions of the positron lifetime spectrometers used.

Spectrometer	1	2	3
Scintillators	Pilot U	Pilot U	BaF_2
(Height)×(diameter) (mm^2)	20×20	35×35	19×19
Time resolution full width at half maximum (FWHM) in (ps)	210	310	190

bient temperature or at −196 °C. In the isochronal annealing treatments annealing times of 20 min were applied with subsequent measurements at room temperature.

B. Positron lifetime measurements and data analysis

For the positron lifetime measurements fast-slow–coincidence spectrometers with either plastic (spectrometers 1 and 2) or BaF_2 scintillators[25] (spectrometer 3) were used. The time drifts did not exceed 2 ps per week.

The experimental time resolutions of the spectrometers (see Table I) that were utilized to perform multicomponent analyses[26] of the measured lifetime spectra (3×10^6–7×10^6 coincidences) were determined by applying the computer program RESOLUTION (Ref. 27) to simple lifetime spectra measured on well-annealed Fe disks with the same sandwich geometry as in the studies of the pellets. The time-resolution functions obtained in this way are considered to be reliable since measurements with the various spectrometers on the same iron specimen yielded the same values of the lifetimes within experimental uncertainty. In decomposing the lifetime spectra by four-component analyses, variances of the numerical fits between 0.98 and 1.15 were obtained.

III. EXPERIMENTAL RESULTS

A general comparison of the positron lifetime in compacted nanometer-sized Fe polycrystals (pellets) with the lifetimes in uncompacted ultrafine Fe crystallites (Fe powder), in the amorphous alloy $Fe_{85.2}B_{14.8}$, and in polycrystalline bulk iron is given in Fig. 3, showing the corresponding lifetime spectra.

The mean positron lifetimes deduced from the initial slope appears to be decisively longer in the pellets [$\bar{\tau}'=(I_1\tau_1+I_2\tau_2)/(I_1+I_2)=274$ ps; see below] than in the amorphous alloy ($\bar{\tau}=142$ ps; see Ref. 23) or the bulk lifetime $\tau_f=106$ ps of the coarse-grained polycrystalline Fe specimen, but shorter than in the ultrafine iron

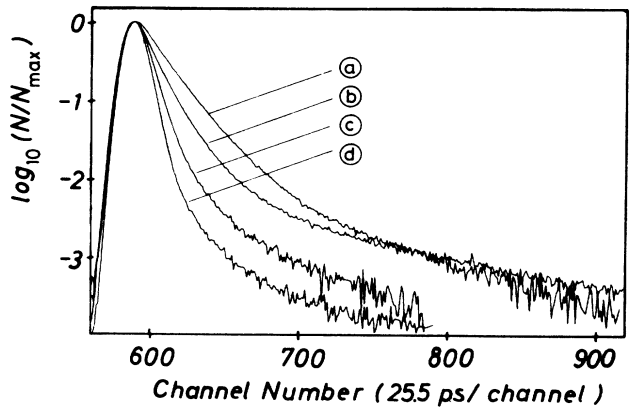

FIG. 3. Positron lifetime spectra on (a) uncompacted Fe powder, (b) a nanocrystalline Fe specimen ($p=56$ MPa), (c) the amorphous $Fe_{85.2}B_{14.8}$ alloy, and (d) polycrystalline bulk iron, with the background of the spectra subtracted.

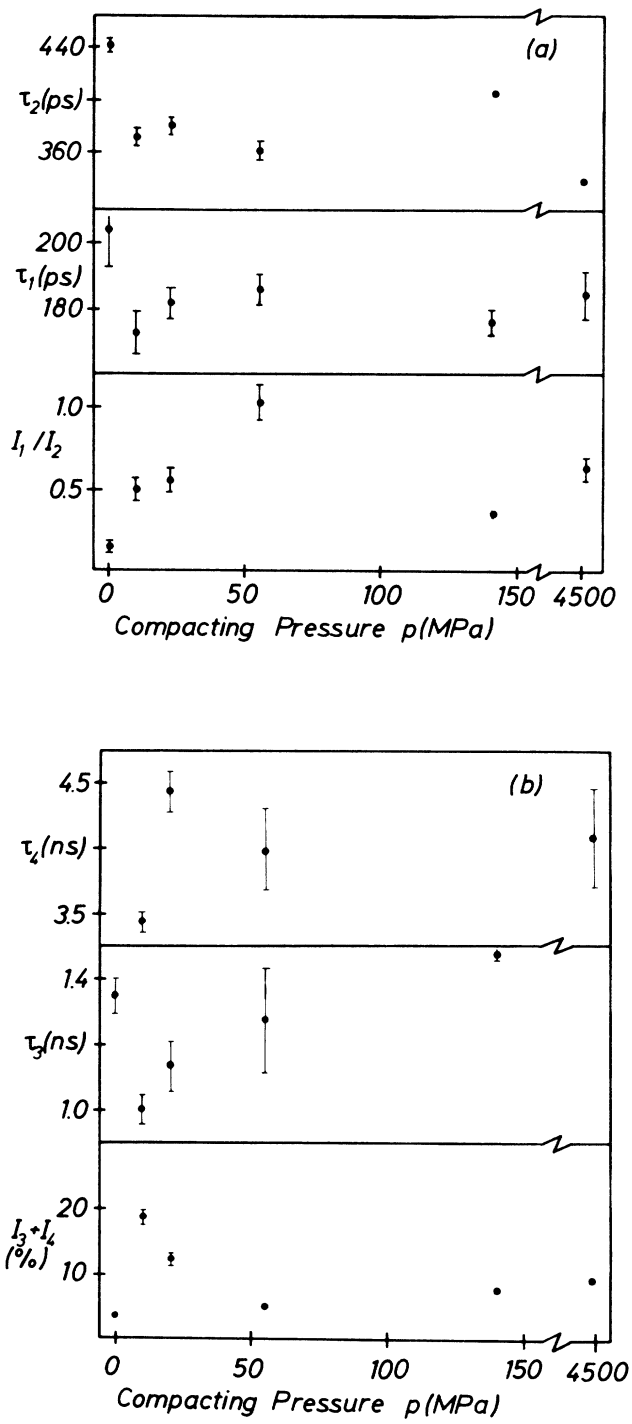

FIG. 4. Time constants and intensities of the components of the lifetime spectra measured on Fe pellets after compacting at room temperature as a function of the compacting pressure p. The values for $p=0$ refer to the measurements on uncompacted nanocrystalline Fe powder. (a) Time constants τ_1 and τ_2 as well as the intensity ratio I_1/I_2. (b) Time constants τ_3,τ_4 and the intensity I_3+I_4. At $p=140$ Pa and 4.5 GPa only one experimental point is given in the diagrams for τ_3 and τ_4, respectively, because only one long-lived component is observed in these spectra.

powder ($\bar{\tau}'=412$ ps). Furthermore, the pellets show an intense long-lived component in contrast to the amorphous or the polycrystalline specimen.

A multicomponent analysis of the lifetime spectrum on nanometer-sized polycrystalline iron (56 MPa, see Fig. 3) reveals the two major components with the intensities I_1 and I_2 (see Fig. 4) and time constants $\tau_1=187\pm4$ ps and $\tau_2=365\pm10$ ps as well as two long-lived contributions of about $\tau_3=1300$ ps and $\tau_4=4000$ ps. These time constants are all considerably longer than the free lifetime in crystalline iron or the main component in amorphous Fe alloys. Short-lived components with lifetimes between 30 and 140 ps were particularly searched for in the numerical analysis of the measurements at ambient temperature, but could not be detected. The above lifetimes and intensities do not change beyond the uncertainty limits (Fig. 4) if, prior to the numerical analysis, corrections for annihilations in the source materials and in the carrier Al foils are subtracted.

The lifetimes τ_1, τ_2, τ_3, and τ_4 are to be considered as characteristic values representing the centers of mass of a certain lifetime distribution. For determining the widths of these distributions, still higher measuring statistics are required. At the highest compacting pressure used in the present experiments only one long-lived component could be resolved [see Fig. 4(b)].

In the Fe-powder specimen the annihilated positrons predominantly have a lifetime of $\tau_2=443\pm5$ ps ($I_2=0.84$). There is a small additional component with about $\tau_1=200$ ps ($I_1=0.13$) and a weak long-lived tail.

A. Influence of the compacting pressure on the positron lifetime spectra

As seen in Fig. 3, the mean positron lifetime $\bar{\tau}'$ decreases considerably by compacting the iron powder to nanometer-sized polycrystalline solids. The numerical analysis of the lifetime spectra measured on pellets after preparation under various pressures [see Figs. 4(a) and 4(b)] shows that this decrease is due to an increase of the intensity I_1 of the short-lived component up to 56 MPa. The time constants τ_1 and τ_2 appear to show only small variations with compacting pressure, which are indicated by the limits given in Table II and which hardly exceed the numerical uncertainties. In Fig. 4 the values of the uncompacted Fe powder are indicated at $p=0$. A decrease of the intensity ratio I_1/I_2 appears to occur at high pressures [Fig. 4(a)]. Furthermore, the intensities of the long-lived components which are high after slight compacting ($I_3+I_4\approx0.19$ for $p=10$ MPa) decrease with increasing pressure.

B. Annealing behavior

Isochronal annealing experiments have been performed on nanocrystalline iron specimens compacted under various pressures (10 MPa, 140 MPa, and 4.5 GPa). Results are given for annealing temperatures $T_a\leq320$ °C. Above this temperature a considerable thermal deformation of the pellets and a geometric change of the sandwich arrangement was observed. The following characteristic features of the annealing behavior common for nanocrystalline iron compacted under various pressures may be pointed out.

(i) The lifetimes $\tau_1=180\pm15$ ps and $\tau_2=360\pm30$ ps which are dominant for all compacting pressures are independent of the annealing temperature within the above limits (see Table II) between 23 and 300 °C [Figs. 5(a) and 6(a)].

(ii) A general increase of the intensities I_3 and I_4 of the long-lived components is observed up to 155 °C. Above this temperature a decrease [Figs. 5(b), 6(b), and 7] is noticed. The mean positron lifetimes of the spectra which are substantially determined by the long-lived components show a maximum at $T_a\sim150$ °C (Fig. 8). This behavior appears to be independent of the compacting pressure.[23]

(iii) The intensities of the long-lived components, I_3 and I_4, measured at room temperature after annealing at $T_a\leq250$ °C slightly increase (within hours) with time.

(iv) Highly compacted pellets (4.5 GPa; Fig. 7) differ in their annealing behavior from specimens with lower compacting pressure [see Figs. 5(b) and 6(b)] by the total annealing out of the long-lived components above 200 °C. Measurements at ambient temperature show these components to be independent of time after annealing above ambient temperature.

C. Variation of the lifetime spectra with temperature

From ambient temperature to -196 °C the intensity I_1 of the short-lived component ($p=56$ MPa) slightly increases at the expense of I_2 without any significant change of τ_1, τ_2, or the long-lived components.

In uncompacted nanocrystalline Fe powder a weak increase of I_1 is observed between -196 and $+125$ °C, whereas τ_2 and I_2 are constant. An increase of I_3 after annealing at 125 °C has been found.

TABLE II. Positron lifetime (in ps) measured on nanocrystalline Fe specimens and uncompacted 6-nm Fe crystallites. The limits given for τ_1 and τ_2 cover the experimental uncertainties and small variations which may occur with the variation of the compacting pressure or during annealing.

	τ_1	τ_2	τ_3	τ_4
Nanocrystalline Fe specimen	180±15	360±30	1200±200	4000±500
Uncompacted 6-nm Fe crystallites	200±20	443±5	1350±50	

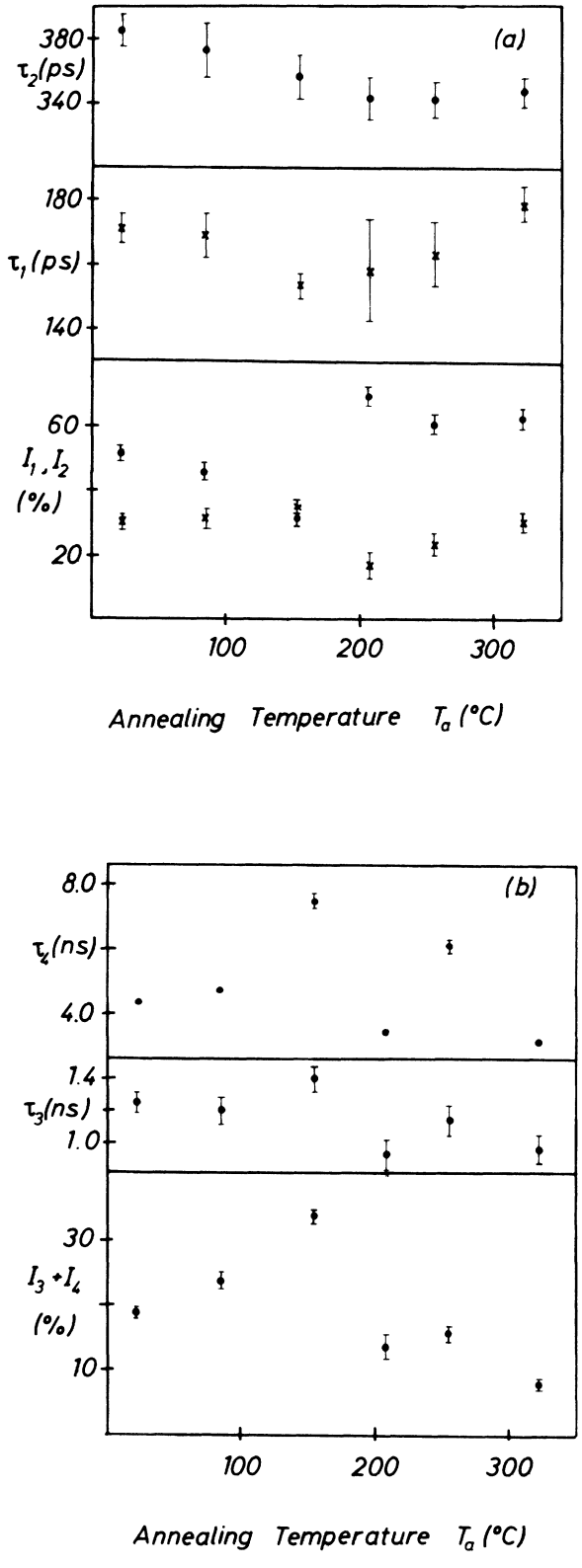

FIG. 5. Lifetime components measured at room temperature after isochronal annealing at the temperature T_a ($t_a = 20$ min) on Fe pellets compacted with $p = 10$ MPa. (a) Time constants τ_1, τ_2 and intensities I_1 ($\times$) and I_2 (●). (b) Time constants τ_3, τ_4 and the intensity $I_3 + I_4$.

D. Positron lifetime measurements on plastically deformed iron

In order to measure the lifetime of positrons trapped at dislocations, a hollow cylinder of the same material as used for the nanometer-sized polycrystalline specimens (Sec. II A) was plastically deformed at room temperature

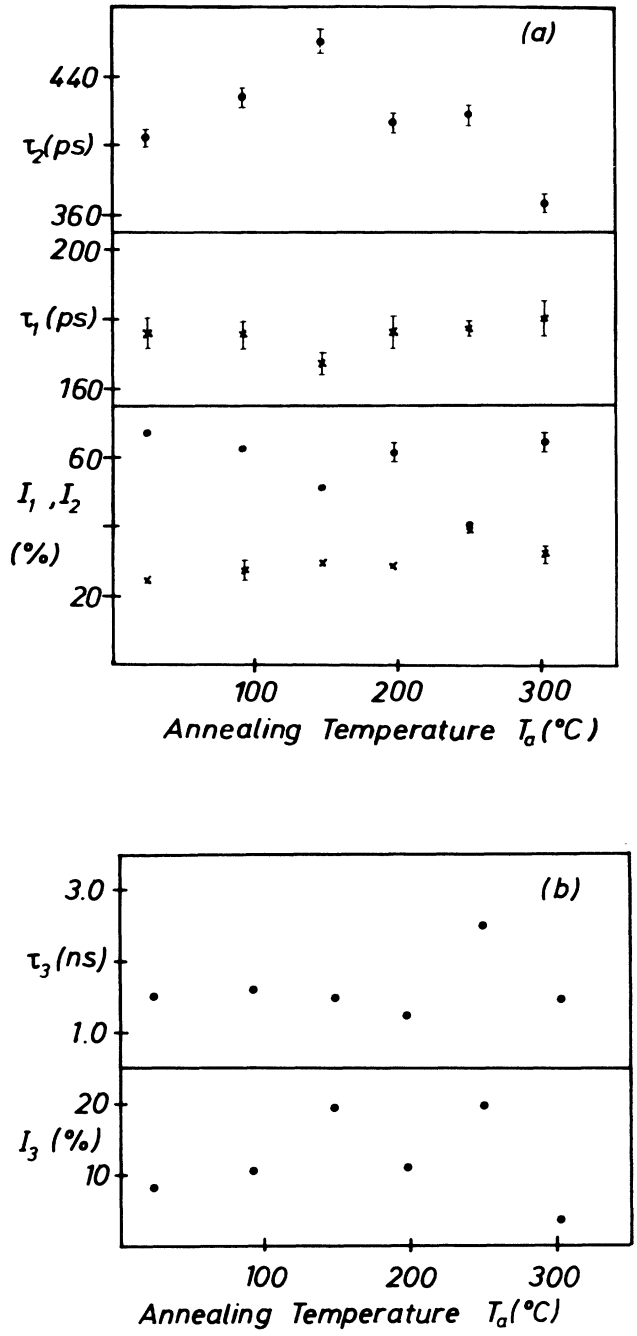

FIG. 6. Lifetime components measured at room temperature after isochronal annealing at the temperature T_a ($t_a = 20$ min) on Fe pellets compacted with $p = 140$ MPa. (a) Time constants τ_1, τ_2 and intensities I_1 ($\times$) and I_2 (●). (b) Time constant τ_3 and intensity I_3.

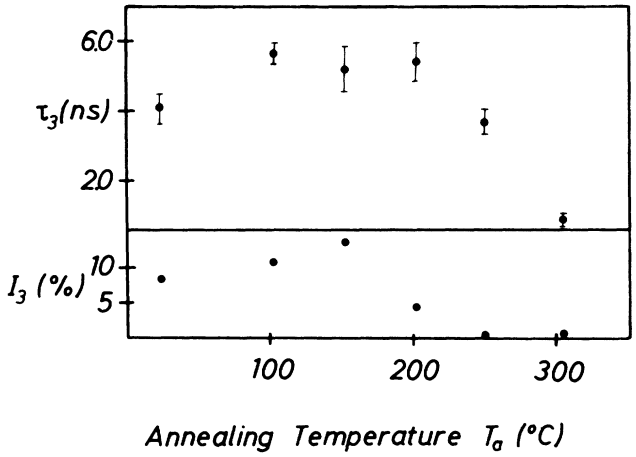

FIG. 7. Time constant τ_3 and intensity I_3 measured at room temperature after isochronal annealing at the temperature T_a ($t_a = 20$ min) on Fe pellets compacted with $p = 4.5$ GPa.

by compression perpendicular to the cylinder axis. The lifetime $\tau_2 = 167 \pm 5$ ps observed with an intensity of $I_2 = 0.65$ is similar to values observed earlier.[28–30] During isothermal measurements at room temperature following plastic deformation, the mean lifetime decreases within 1 d by about 8%, indicating the recovery of point-defect positron traps which exist in addition to dislocations. At present, it is not clear what the nature of the trapping site on a dislocation really is. According to the detailed investigation of Tanigawa *et al.*,[31] jogs or vacancies bound to dislocations may act as traps.

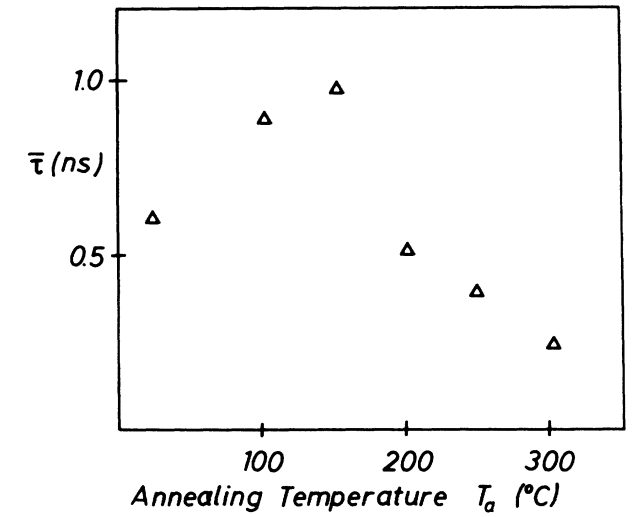

FIG. 8. Mean lifetimes $\bar{\tau}$ measured at room temperature after isochronal annealing at the temperature T_a ($t_a = 20$ min) on Fe pellets compacted with $p = 4.5$ GPa.

IV. DISCUSSION

Considering the analysis of the positron lifetime spectra (Fig. 4), we find that all positrons injected into the nanometer-sized polycrystalline Fe specimen are annihilated with lifetimes clearly longer than in the delocalized free state ($\tau_f = 106$ ps) in a bulk iron crystal. Thus we conclude that all positrons are localized at traps before annihilation. In this case of saturation trapping only a rough estimate of the concentration ratios of different types of traps can be given. In the following the positron lifetimes τ_1 ("short"), τ_2 ("intermediate"), as well as τ_3 and τ_4 ("long") will be discussed and an association with the structural elements of the nanocrystalline iron material will be attempted.

A. Positron annihilation in the crystalline interfaces

The shortest positron lifetime, $\tau_1 = 180 \pm 15$ ps, which has been observed in all nanometer-sized polycrystalline Fe specimens with considerable intensity, is very similar to the lifetime $\tau_{1v} = 175$ ps of positrons in monovacancies in Fe bulk crystals.[30,32] A slightly lower value, $\tau_d = 167$ ps (see Sec. III D), is correlated to positron annihilation at dislocations.

We attribute the time constant τ_1 to positron trapping and annihilation at free volumes of approximately the size of a monovacancy in the crystallite interfaces of the nanocrystalline material (see Fig. 9) on the basis of the following evidence.

Free monovacancies within the crystallites or vacancy-carbon pairs (which may be produced due to impurity contamination during specimen preparation) are

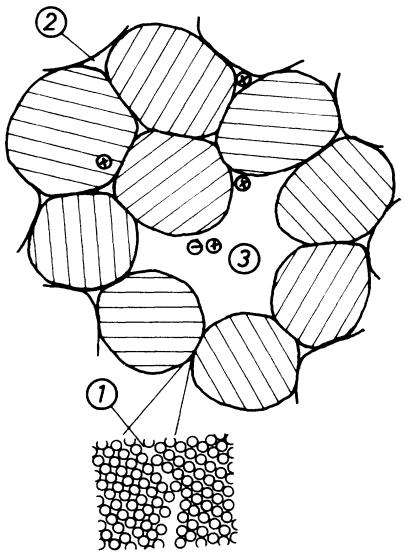

FIG. 9. Schematic two-dimensional arrangement of crystallites in a nanocrystalline material. The hatching indicates the orientation of lattice planes. The atomic structure of the interface is shown schematically in the inset. The various annihilation sites are attributed to the positron lifetimes (1) $\tau_1 = 180 \pm 15$ ps, (2) $\tau_2 = 360 \pm 30$ ps, and (3) $1000 \leq \tau_{3,4} \leq 5000$ ps, as discussed in the text.

not likely as positron traps since these defects are assumed to recover in crystalline iron at temperatures below $T_a = 320\,^{\circ}\mathrm{C}$.[32–34]

The interpretation of τ_1 by vacancy-size traps in the crystallite boundaries is supported by the increase in the intensity I_1 with the compacting pressure. A higher compacting pressure is assumed to increase the interfacial area and thereby the overall density of vacancy-size traps. In a similar way Mössbauer experiments[11] show—in addition to the characteristic spectrum of α-iron—with increasing compacting pressure an intensity increase of a new broadened component which is attributed to a broad distribution of the hyperfine fields at the Mössbauer probe due to a wide distribution of interatomic distances. Such a distribution of interatomic distances in the interfaces has been also evidenced by x-ray-diffraction experiments and correlated simulation calculations.[7] Therefore, the observation of vacancy-size free volumes by positron lifetime measurements in the nanocrystalline interfaces is in good accordance with an atomic structure of the interfaces without short-range order and with a wide interatomic distance distribution.

In the nanocrystalline iron no lifetimes $\tau_f \leq \tau \leq 180$ ps characteristic for positrons trapped at free volumes smaller than vacancies such as in amorphous metals[35] could be observed. This could mean that smaller free volumes which may exist in the interfaces do not effectively trap positrons particularly in competition with strong traps of vacancy size. Some indication for positron trapping at "shallow" traps at low temperatures and thermally activated detrapping at higher temperatures may be deduced from the temperature behavior of the ratio I_1/I_2 which decreases with increasing measuring temperatures between $-196\,^{\circ}\mathrm{C}$ and ambient temperature (see Sec. III C).

In a few investigations performed on fine-grained Zn-Al alloys in order to study grain-boundary or phase-boundary properties,[36–38] positron lifetimes similar to those of lattice vacancies in the pure metals have been reported. However, in contrast to single-component nanocrystalline materials, the interpretation of these results may be hindered by positron trapping at stable vacancy-dopant complexes[37,38] or precipitates.[37] Furthermore, in these alloys with grain sizes $\geq 1\ \mu$m, positron trapping at dislocations may occur.

In the case of the nanocrystalline iron specimens the positron lifetime $\tau_1 = 180$ ps seems unlikely to be due to positron trapping at dislocations, yielding a considerably smaller value (see Sec. III D).

B. The intermediate lifetime

The lifetime $\tau_2 = 360 \pm 30$ ps observed with high intensity in the lifetime spectra on nanocrystalline iron is attributed to positrons trapped at free volumes at the intersections of two or three crystallite interfaces (see Fig. 9). These intersections may be considered to have shapes like pipes or microvoids, respectively. In bulk iron crystals the above lifetime value is expected for agglomerates of about 10–15 vacancies[39] with a spherical diameter of about 0.6 nm. The presence of free volumes of this size may be plausible if we assume that the atomic positions near the center of such a boundary intersection are unstable in the case of strongly differing orientations of the adjoining crystallites.

In the above interpretation the persistance of the intermediate lifetime during annealing (see Sec. IV D) and initial crystallite growth[8] finds a natural explanation because such intersection sites continue to exist and can act as positron traps as long as the crystallites are considerably smaller than the positron diffusion length.

We cannot exclude that specific trapping sites in larger voids such as surface defects stable to the present annealing procedure may contribute to the intermediate-lifetime component. Particularly, edges and corners at the periphery of a larger void (one or several crystallites missing, see Fig. 9) may act as positron traps with lifetimes similar to that of interfacial intersections.

Some comments should be made concerning the concentration of positron traps in nanometer-sized polycrystalline Fe. No short lifetime, $\tau_0 < \tau_f$, could be detected in the spectra where

$$\tau_0 = \left[\frac{1}{\tau_f} + \sum_i \sigma_i C_i \right]^{-1} \tag{1}$$

is the residence time of positrons in the delocalized lattice state. The C_i denote the concentrations of various types, i, of traps, and the σ_i denote the corresponding specific trapping rates. A negligible value $\tau_0 \ll \tau_f$ appears to be reasonable because, due to their long diffusion length $L_+ \approx 100$ nm in crystalline bulk metals,[40] the thermalized positrons may nearly quantitatively attain the surface of the 6-nm crystallites in the nanocrystalline Fe material and be trapped at interfacial vacancies, microvoids, or larger voids.

In this case of saturation trapping the trapping rates $\sigma_i C_i$, which are correlated to the intensities by

$$I_i = \sigma_i C_i / (1/\tau_0 - 1/\tau_i) \tag{2}$$

according to the trapping model, cannot be determined experimentally. However, ratios like

$$\sigma_1 C_1 / \sigma_2 C_2 \approx I_1 / I_2 \tag{3}$$

can be derived. Assuming equal trapping rates per unit area for interfaces with vacancy defects between the crystallites (see Sec. IV A) or for the crystallite-microvoid interfaces the area ratio of the two types of interfaces may be estimated to 0.5–1 [see Fig. 4(a)] using the experimental values for I_1/I_2. This is in reasonable agreement with the area ratio of these interface types in increasingly compacted 6-nm crystallites.

The decrease of I_1/I_2 for higher pressures ($p \geq 140$ MPa) may be due to a saturation behavior of the formation of new interfaces and a decrease of the number of va-

cancylike free volumes in the interfaces arising from interatomic relaxation processes during the plastic deformation of crystallites at high compaction pressures.

C. The long lifetimes and positronium formation

Positron lifetimes longer than 1 ns, as observed in the nanocrystalline Fe specimens ($\tau_3 \approx 1300$ ps, $\tau_4 \approx 4000$ ps) with intensities between 10% and 30% [see Figs. 4(b), 5(b), 6(b), and 7], indicate the formation of orthopositronium (o-Ps) at the internal surfaces of larger voids. Pores with diameters of about 1 μm have been observed by optical microscopy. The free lifetime $\tau = 142$ ns of o-Ps in vacuum is assumed to be reduced to a few nanoseconds by transitions to the para-positronium state (p-Ps, $\tau = 123$ ps) due to spin-conversion and pickoff processes when interacting with the internal surfaces. The efficiency of these processes, and therefore the o-Ps *lifetime* in the nanocrystalline Fe pellets, is expected to be determined by the structure and the contamination[16] of these surfaces. The size of the voids may influence the long-time constants via the collision rate of the Ps atoms with the wall.[41] In the case of iron, magnetic stray fields at the surfaces may also contribute to the spin conversion of o-Ps. The *intensity* of the long-lived components is governed by the positron work function and the Ps surface binding energy, which both sensitively depend[42,43] on the deposition of foreign atoms on the surface. The variety of processes which may affect the long-lived components may naturally explain the appearance of a lifetime distribution which may be represented in the present case by two components after low compacting pressures. The observation of a single nanosecond component in highly compacted specimens [4.5 GPa, see Fig. 4(b)] would then indicate one single type of void, the nature of which cannot be clarified by means of the present measurements.

In the present experiments on nanocrystalline iron evidence for the influence of surface impurities on Ps formation may be deduced from the annealing behavior of the long-lived components (see Sec. IV D).

The much lower intensities of the long-lived components measured on uncompacted iron powder compared to the nanocrystalline pellets [see Fig. 4(b)] may originate from different surface structures of the loose powder and the voids in compacted pellets. In particular, a hydrogen contamination of the powder may have occurred since after preparation this specimen has been melted off in a quartz vial which at high temperatures is permeable to the hydrogen of the melting flame. In contrast to that, the nanocrystalline pellets have been stored in Duran glass vials unpermeable to hydrogen.

The interpretation of the reduction of the long-lived component in the powder by hydrogen contamination is supported by the experiments of Mogensen *et al.*,[16] who observed an increased conversion ratio from o-Ps to p-Ps due to hydrogen adsorption on Fe microcrystals.

As discussed above, Ps formation as observed in nanocrystalline materials depends on a number of various parameters and only a qualitative interpretation can be suggested at present. However, these experiments show that high-resolution lifetime measurements on nanocrystalline materials may represent a useful method to investigate solid surfaces and positronium formation. Controlled gas absorption and desorption may further clarify these questions.

D. Thermal annealing and structural stability

Two main results of the annealing experiments on Fe pellets of all compaction states investigated may be summarized.

(i) The components with lifetimes of $\tau_1 = 180$ ps and $\tau_2 = 360$ ps persist up to 320 °C without significant changes [Figs. 5(a), 6(a), and Table II].

(ii) The intensities of the components with lifetimes longer than 1 ns increase up to 150 °C and tend to anneal out above 300 °C [Figs. 5(b), 6(b), 7 and 8].

Electron-microscopic studies of Hort[8] on nanocrystalline iron show that no significant growth of the 6-nm crystallites occurs below 200 °C. At 300 °C a mean particle diameter of 40 nm is attained. Assuming a mean diffusion length of $L_+ = 100$ nm, positrons are still expected to diffuse with high probability from the interior of the crystallites into the traps at interfaces and surfaces without measurable annihilation in the bulk state. Thus we can understand that the component τ_1 attributed to vacancy-size positron traps in the interfaces does not change visibly with annealing as long as the diffusion length L_+ clearly exceeds the crystallite size.

The stability of the intermediate component with $\tau_2 = 360$ ps which is assigned to microvoids at boundary intersections may be interpreted in a similar way because it does not anneal out up to 320 °C.

No significant variations of the positron lifetimes τ_1 and τ_2 exceeding the given uncertainty limits were observed with varying compacting pressure or annealing temperature. This means that the sizes of the corresponding free volumes of the positron traps are independent of compacting pressure or the present annealing treatment within the limits given in Table II and that these free volumes have to be considered as structural elements of the nanocrystalline Fe specimens.

The annealing of the long-lived components is obviously more complicated since the formation and the lifetime of positronium depends on the void properties in detail. So, the increase of $I_3 + I_4$ up to 150 °C may be attributed to a contamination of the void walls by diffusing gases. A similar interpretation has been given for increased positronium formation in voids in Nb and Ta (Ref. 44) during annealing.

Recovery of surface defects as reported in the case of Cu layers on W surfaces[45] may also contribute to the increase of Ps formation in the voids.

The decrease of $I_3 + I_4$ at higher annealing temperatures may originate from gas desorption from the void surface. The slow reincrease (within hours) observed at room temperature after annealing below 200 °C is then attributed to readsorption of gases from the closed specimen-container volume onto the void walls. On the other hand, crystallite growth[8] above 200 °C as mentioned above will lead to void shrinkage and an intensity

decrease of the long-lived components. This is expected particularly in the case of highly compacted materials with a small total void volume where the long-lived components anneal out at $T_a \geq 250$ °C [Figs. 6(b) and 7].

In conclusion, the present results show that the vacancy-size traps in the interfaces and the microvoids at the intersections of the interfaces have to be considered as structural elements of the nanocrystalline material. The decrease of the positronium fraction during annealing indicates shrinkage of larger voids due to material transport.

As discussed above, impurity contamination may affect o-Ps formation in larger voids. It cannot be excluded that in the present specimens the nature of the traps giving rise to the positron lifetimes τ_1 and τ_2 may be influenced by such contaminations. Preparation of specimens of highest purity, ultrahigh-vacuum handling, and careful characterization have to be aimed at in future experiments.

Positron-annihilation techniques become more and more valuable for the investigation of surfaces and interfaces by using slow-positron beams.[45] Evidently, studies of nanocrystalline materials may supply similar information since positrons with a wide energy distribution from decay sources are "moderated" within the specimens with high moderation efficiency and trapped at interfaces or internal surfaces. Besides that, in studies on nanocrystalline specimens positron lifetime measurements with high time resolution may be utilized for identifying the annihilation states.

Gas adsorption on surfaces may be studied by diffusing gases into the nanocrystalline specimens. Furthermore, depth profiling as performed in slow-positron experiments may be simulated in measurements on nanocrystalline specimens by increasing the crystallite size.

E. Positron lifetime in nanocrystalline iron powder

Since the thermalized positrons can diffuse to the surface of the 6-nm crystallites in times much shorter than their free lifetime τ_f, the dominant time constant, $\tau_2 = 443$ ps, in the loosely packed powder is attributed to annihilation at the surfaces, which in this case act as positron traps. The question is whether the positrons are annihilated in a Ps state outside the crystallites or in a low-density surface electron gas. Earlier measurements on 10-nm Ni (Ref. 13) or 100-nm Fe (Ref. 12) powders show lifetimes similar to those noted in the present experiments. A narrow electron momentum distribution derived from angular-correlation measurements of the annihilation radiation (ACAR) by Tsuchiya *et al.*[14] on 10-nm Fe crystallites is considered as evidence for p-Ps formation by the authors. Positronium formation on metal surfaces is well known from slow-positron experiments[46] and can be detected by 3γ annihilation of o-Ps. The presently observed lifetime τ_2 in the nanocrystalline powder which is smaller than predicted for the o-p-conversion limit (500 ps, see Sec. IV C) may be attributed to additional pickoff processes near the surface.

The positron-annihilation data available for surfaces at present may, on the other hand, be also interpreted by annihilation of positrons trapped near the surface in a low-density electron gas with Fermi momenta decreasing outside the surface. The positron surface lifetime ($\tau_s = 580$ ps) obtained from slow-positron experiments on Al surfaces[47] had been studied[48] by calculating the surface positron wave function and, finally, rough agreement with the experimental results could be obtained by refraining from the local-density approximation,[49] which is used for lifetime calculations in the bulk metal.[48] The lifetime $\tau_2 = 443$ ps measured in ultrafine Fe powder may be compatible with the interpretation based on surface annihilation states if the higher electron density in iron as reflected by the lifetime $\tau_f = 106$ ps smaller than in Al ($\tau_f = 163$ ps; Ref. 17) is taken into account.

From positron age-momentum measurements[15] on Ag and Au powders (70 nm) indication for annihilation from Ps and positron states is derived. Here, positronium annihilation far off the surface may be detected which can be separated from the surface annihilation in the case of measuring the two-dimensional angular correlation of the annihilation radiation (2D ACAR).[50,51]

The short lifetime, $\tau_1 = 204 \pm 18$ ps, measured in nanocrystalline iron powder with low intensity [see Fig. 4(a)] is attributed in a similar way as in Sec. IV A to positron trapping in interfacial free volumes, which—in the case of loosely packed powder—may have a slightly larger size than lattice vacancies. Measurable trapping at this type of site is expected even for the low interfacial density of loose powder due to the high diffusivity of positrons on surfaces.[48]

The weak long-lived component [Fig. 4(b)] is attributed to formation of o-Ps, which annihilates with a reduced lifetime due to collisions with the crystallites.

The present results and the tentative model demonstrate that positron lifetime spectroscopy can specifically contribute to the understanding of the structural properties of nanometer-sized polycrystalline materials. In order to test the present picture, variation of the crystallite size during preparation or by further annealing, as well as diffusion and surface deposition of dopants, are desirable.

V. SUMMARY AND CONCLUSIONS

Studies of positron lifetime spectroscopy have been performed on nanometer-sized polycrystalline Fe specimens with a mean crystallite size of 6 nm.

(i) The positron lifetime $\tau_1 = 180$ ps gives first evidence for free volumes in crystallite interfaces which have approximately the size of a lattice vacancy. This is in agreement with a wide distribution of atomic distances and vanishing short-range order suggested by Gleiter *et al.*[2] for the interfacial phase of the nanocrystalline material and is in contrast to crystalline and amorphous materials.

(ii) The lifetime $\tau_2 = 360$ ps is attributed to microvoids at the intersections of crystallite interfaces.

(iii) According to the annealing experiments, the interfacial vacancies and the microvoids are to be considered as structural elements of the nanocrystalline material.

(iv) Saturation trapping of positrons indicates a high concentration of trapping centers.

(v) The long-lived annihilation components between 1

and 5 ns observed in nanometer-sized polycrystalline Fe pellets are characteristic for Ps formation at the surfaces of larger voids.

(vi) Polycrystalline materials with nanometer-size crystallites are expected to represent convenient systems for investigating surfaces and interfaces by positron lifetime spectroscopy.

ACKNOWLEDGMENTS

We thank Dr. P. Marquardt for contributions in the early stage of the experiments. The continuous support of Professor A. Seeger is acknowledged. The authors are indebted to Professor R. J. Zaworski (deceased) for critically reading the manuscript.

[1]H. Gleiter and P. Marquardt, Z. Metallkund. **75**, 263 (1984).
[2]R. Birringer, H. Gleiter, H.-P. Klein, and P. Marquardt, Phys. Lett. **102A**, 365 (1984).
[3]R. Birringer, U. Herr, and H. Gleiter, Trans. Jpn. Inst. Met. Suppl. **27**, 43 (1986).
[4]Proceedings of the International Conference on Frontiers of Glass Science [J. Non-Cryst. Solids **42**, 1 (1980)].
[5]*Rapidly Quenched Metals*, edited by S. Steeb and H. Warlimont (North-Holland, Amsterdam, 1985).
[6]D. Shechtman, I. Blech, D. Gratias, and J. W. Cahn, Phys. Rev. Lett. **53**, 1951 (1984).
[7]X. Zhu, R. Birringer, U. Herr, and H. Gleiter, Phys. Rev. B **35**, 9085 (1987).
[8]E. Hort, Diploma thesis, Universität des Saarlandes, Saarbrücken, 1985.
[9]J. Rupp and R. Birringer, Phys. Rev. B **36**, 7888 (1987).
[10]T. Haubold, Diploma thesis, Universität des Saarlandes, Saarbrücken, 1986.
[11]U. Herr, J. Jing, R. Birringer, U. Gonser, and H. Gleiter, Appl. Phys. Lett. **50**, 472 (1987).
[12]R. Paulin and R. Ripon, Appl. Phys. **4**, 343 (1974).
[13]S. Noguchi and Y. Miyata, in *Positron Annihilation*, edited by R. R. Hasiguti and K. Fujiwara (Japan Institute of Metals, Sendai, 1979), p. 879.
[14]Y. Tsuchiya, S. Noguchi, and M. Hasegawa, Philos. Mag. B **39**, 181 (1979).
[15]Y. Matsuoka, S. Terakado, and S. Tanigawa, Phys. Status Solidi B **125**, 823 (1984).
[16]O. E. Mogensen, M. Eldrup, S. Mørup, J. W. Ørnbo, H. Topsøe, in *Positron Annihilation*, edited by P. C. Jain, R. M. Singru, and K. P. Gopinathan (World Scientific, Singapore, 1985), p. 980.
[17]H. E. Schaefer, R. Gugelmeier, M. Schmolz, and A. Seeger, in *Microstructural Characterization of Materials by Non-Microscopical Techniques*, edited by N. Hessel Andersen *et al.* (Risø National Laboratory, Roskilde, 1984), p. 489.
[18]W. Weiler and H. E. Schaefer, J. Phys. F **15**, 1651 (1985).
[19]H. E. Schaefer and R. Würschum, Phys. Lett. **119A**, 370 (1987).
[20]H. E. Schaefer, Phys. Status Solidi A **102**, 47 (1987).
[21]H. E. Schaefer, R. Würschum, R. Schwarz, D. Slobodin, and S. Wagner, Appl. Phys. A **40**, 145 (1986).
[22]C. G. Granqvist and R. A. Buhrmann, J. Appl. Phys. **47**, 2200 (1976).
[23]R. Würschum, Diploma thesis, Stuttgart University, 1985.
[24]I. Dézsi, Z. Kajcsos, and B. Molnár, Nucl. Instrum. Methods **141**, 401 (1977).
[25]W. Bauer, J. Major, W. Weiler, K. Maier, and H. E. Schaefer, in *Positron Annihilation*, Ref. 16, p. 804.
[26]P. Kirkegaard and M. Eldrup, Comput. Phys. Commun. **7**, 401 (1974).
[27]P. Kirkegaard, M. Eldrup, O. E. Mogensen, and D. J. Pedersen, Comput. Phys. Commun. **23**, 975 (1981).
[28]F. Van Brabander, D. Segers, M. Dorikens, and L. Dorikens-Vanpraet, in *Positron Annihilation*, edited by P. G. Coleman, S. C. Sharma, and L. M. Diana (North-Holland, Amsterdam, 1982), p. 472.
[29]P. Hautojärvi, A. Vehanen, and V. S. Mikhalenkov, Appl. Phys. **11**, 191 (1976).
[30]A. Vehanen, P. Hautojärvi, J. Johansson, J. Yli-Kauppila, and P. Moser, Phys. Rev. B **25**, 762 (1982).
[31]S. Tanigawa, K. Ito, S. Terakado, A. Morisue, S. Fujii, and Y. Jwase, in *Positron Annihilation*, Ref. 16, p. 288.
[32]P. Hautojärvi, T. Judin, A. Vehanen, J. Yli-Kauppila, J. Johansson, J. Verdone, and P. Moser, Solid State Commun. **29**, 855 (1979).
[33]H. E. Schaefer, K. Maier, M. Weller, D. Herlach, A. Seeger, and J. Diehl, Scr. Metall. **11**, 803 (1977).
[34]M. Mondino and A. Seeger, Scr. Metall. **11**, 817 (1977).
[35]N. Shiotani, in *Positron Annihilation*, Ref. 28, p. 561.
[36]B. T. A. McKee, G. J. C. Carpenter, J. F. Watters, and R. J. Schultz, Philos. Mag. A **41**, 65 (1980).
[37]G. Dlubek, O. Brümmer, P. Hautojärvi and J. Yli-Kauppila, Philos. Mag. A **44**, 239 (1981).
[38]C. Hidalgo, N. de Diego, and F. Plazaola, Phys. Rev. B **31**, 6941 (1985).
[39]M. J. Puska and R. M. Nieminen, J. Phys. F **13**, 333 (1983).
[40]A. P. Mills and R. J. Wilson, Phys. Rev. A **26**, 490 (1982).
[41]R. N. West, A. Alam, P. A. Walters, and J. D. McGervey, in *Positron Annihilation*, Ref. 28, p. 337.
[42]K. G. Lynn and H. Lutz, Phys. Rev. B **22**, 4143 (1980).
[43]A. P. Mills, Jr., Solid State Commun. **31**, 623 (1979).
[44]M. Hasegawa, E. Kuramoto, K. Kitajima, M. Hirabayashi, Y. Ito, T. Takeyama, H. Takahashi, and S. Ohnuki, in *Positron Annihilation*, Ref. 28, p. 425.
[45]P. J. Schultz, K. G. Lynn, W. E. Frieze, and A. Vehanen, Phys. Rev. B **27**, 6626 (1983).
[46]A. P. Mills, Jr., Phys. Rev. Lett. **41**, 1828 (1978).
[47]K. G. Lynn, W. E. Frieze, and P. J. Schultz, Phys. Rev. Lett. **52**, 1137 (1984).
[48]R. M. Nieminen and M. J. Puska, Phys. Rev. Lett. **50**, 281 (1983).
[49]R. M. Nieminen, M. J. Puska, and M. Manninen, Phys. Rev. Lett. **53**, 1298 (1984).
[50]K. G. Lynn, A. P. Mills, Jr., R. N. West, S. Berko, K. F. Canter, and L. O. Roellig, Phys. Rev. Lett. **54**, 1702 (1985).
[51]R. W. Howell, M. F. Fluss, I. J. Rosenberg, and P. Meyer, in *Positron Annihilation*, Ref. 16, p. 801.